

## Submillimeter Array Observations of CS J=14–13 Emission from the Evolved Star IRC+10216

K.H. Young<sup>1</sup>, T.R. Hunter<sup>1</sup>, D.J. Wilner<sup>1</sup>, M.A. Gurwell<sup>1</sup>,  
J.W. Barrett<sup>1</sup>, R. Blundell<sup>1</sup>, R. Christensen<sup>2</sup>, D. Fong<sup>2</sup>, N. Hirano<sup>3</sup>, P.T.P. Ho<sup>1,3</sup>, S.Y. Liu<sup>3</sup>, K.Y. Lo<sup>3,5</sup>, R. Martin<sup>3</sup>, S. Matsushita<sup>3</sup>, J.M. Moran<sup>1</sup>, N. Ohashi<sup>3</sup>, D.C. Papa<sup>1</sup>, N. Patel<sup>1</sup>, F. Patt<sup>3</sup>, A. Peck<sup>2</sup>, C. Qi<sup>1</sup>, M. Saito<sup>1,4</sup>, A. Schinckel<sup>2</sup>, H. Shinnaga<sup>2</sup>, T.K. Sridharan<sup>1</sup>, S. Takakuwa<sup>2</sup>, C.E. Tong<sup>1</sup>, D.V. Trung<sup>3</sup>

dwilner@cfa.harvard.edu

### ABSTRACT

We present imaging observations of the evolved star IRC+10216 in the CS J=14–13 line at 685.4 GHz and associated submillimeter continuum at  $\sim 2''$  resolution made with the partially constructed Submillimeter Array. The CS J=14–13 line emission from the stellar envelope is well resolved both spatially and spectrally. The strong central concentration of the line emission provides direct evidence that CS is a parent molecule that forms close to the stellar photosphere, in accord with previous images of the lower excitation CS J=2–1 line and inferences from unresolved observations of vibrationally excited transitions. The continuum emission is dominated by a compact, unresolved component, consistent with the photospheric emission, that accounts for  $\sim 20\%$  of the broadband 450  $\mu\text{m}$  flux. These are the first interferometer imaging observations made in the semi-transparent 450  $\mu\text{m}$  atmospheric window.

*Subject headings:* circumstellar matter — stars: individual (IRC+10216) — astrochemistry — techniques: interferometric

---

<sup>1</sup>Harvard-Smithsonian Center for Astrophysics, 60 Garden Street, Cambridge, MA 02138, USA

<sup>2</sup>Harvard-Smithsonian Center for Astrophysics, Submillimeter Array, 645 N. A'ohoku Place, Hilo, HI 96721, USA

<sup>3</sup>Academia Sinica Institute of Astronomy & Astrophysics, P.O. Box 23-141, Taipei, Taiwan, 106, R.O.C.

<sup>4</sup>National Astronomical Observatory of Japan, 2-21-1 Osawa, Mitaka, Tokyo 181-8588, Japan

<sup>5</sup>National Radio Astronomy Observatory, 520 Edgemont Road, Charlottesville, VA 22903, USA

## 1. Introduction

The nearby carbon star IRC+10216 (CW Leo, IRAS 09452+1330) is surrounded by a dusty, expanding envelope with relatively simple geometry and kinematics that has been the subject of many studies of astrochemical processes. A rich chemistry develops in the envelope as gas is lost from the star at a high rate ( $\sim 3 \times 10^{-5} M_{\odot} \text{ yr}^{-1}$ , Crosas & Menten 1997) and is modified by thermodynamic equilibrium and non-equilibrium reactions, photochemical reactions, ion-molecule reactions, and the condensation of dust grains. The range of physical conditions in the envelope make it especially well suited to observations of rotational emission lines from molecules, and numerous species have been identified in spectral scans at millimeter and submillimeter wavelengths (e.g. Cernicharo, Guelin & Kahane 2000; Groesbeck, Phillips & Blake 1994, Avery et al. 1992).

The close proximity ( $\sim 150$  pc) and copious mass loss of IRC+10216 allows studies of the circumstellar envelope on a wide range of size scales. On the largest scales, an extensive envelope of dust (Mauron & Huggins 1999) and gas (Fong, Meixner & Shah 2003) has been found to extend to  $\sim 0.15$  pc ( $\sim 3'3$ ) in radius. On much smaller scales, interferometric imaging at millimeter wavelengths has revealed the spatial distribution of molecular species within the central arcminute (e.g. Bieging & Tafalla 1993, Guelin, Lucas & Cernicharo 1993, Lucas & Guelin 1999). Parent molecules are found to be centrally peaked (e.g. SiS, HCN), while daughter molecules are found with shell distributions (e.g. CN, C<sub>2</sub>H, HNC). High angular resolution is especially important for imaging lines of high excitation that emerge from the innermost regions of the envelope, where the temperatures and densities are highest.

Since the high excitation rotational lines of many common molecules lie at short submillimeter wavelengths, the Submillimeter Array<sup>1</sup> (SMA) opens new possibilities for probing physical conditions and chemistry by enabling imaging observations with arcsecond resolution. In this *Letter*, we present observations of IRC+10216 in CS J=14–13 emission made with the partially constructed SMA (Ho, Moran & Lo 2004). These are the first interferometer images from observations in the atmospheric window centered near 450  $\mu\text{m}$ , where  $\sim 30\%$  or better transmission occurs at high, dry sites like the summit of Mauna Kea a significant fraction of the time. They build on the pioneering efforts of Carlstrom et al. (1994), who obtained fringes on the nearby single baseline between the Caltech Submillimeter Observatory and the James Clerk Maxwell Telescope. The results provide constraints on sulfur chemistry in the inner wind of the IRC+10216 prototype carbon-rich circumstellar envelope.

---

<sup>1</sup>The Submillimeter Array is a joint project between the Smithsonian Astrophysical Observatory and the Academia Sinica Institute of Astronomy and Astrophysics, and is funded by the Smithsonian Institution and the Academia Sinica.

## 2. Observations

We observed IRC+10216 on 10 December 2002 with the SMA when three of the 6 meter diameter antennas were equipped with receivers for the “600–700 GHz” frequency band. The weather was very good, with 225 GHz atmospheric opacity of 0.035 measured at the nearby Caltech Submillimeter Observatory through the night, or  $\sim 0.7$  at the SMA observing frequency. Table 1 summarizes the observational parameters. We adopt the CS J=14–13 line rest frequency of 685.435923 GHz, recently calculated from newly determined spectroscopic constants (Gottlieb, Myers & Thaddeus 2003). The SMA observations provided three independent baselines ranging from 14 to 25 meters in length, resulting in  $\sim 2''$  resolution.

A major difficulty for interferometric imaging at these high frequencies is the lack of sufficiently strong sources with known structure for the derivation of complex gains to track instrumental phase drifts and atmospheric fluctuations. In particular, nearly all of the point-like quasars are too weak for the SMA to detect at shorter wavelengths in a few minutes of integration time. Compact thermal sources such as planetary moons or asteroids provide one alternative. For these observations, we took advantage of the close proximity of Jupiter to IRC+10216 in the sky ( $< 7$  degrees). While Jupiter was far too large to be a suitable calibrator (diameter  $40''$ ), the Galilean moons were only slightly resolved on these baselines, and high signal-to-noise observations of Callisto (diameter  $1''.4$ ) could be efficiently interleaved with those of IRC+10216. Jupiter was located well outside the small SMA field of view during the observations of Callisto, and the data show no evidence for any contamination from the planetary emission. IRC+10216 was tracked over the hour angle range  $-4\text{h}$  to  $+4\text{h}$ . The predicted flux of Callisto varied by less than 10% due to resolution effects.

The partially complete digital correlator was configured with four overlapping “chunks”, each of 104 MHz bandwidth and 128 channels, with the CS J=14–13 line centered in one of them. A calibration of the bandpass shape was obtained from observations of Mars. The system temperatures ranged from 1200 to 2200 K (DSB). The absolute flux scale was set assuming a full disk flux of 55 Jy for Callisto, based on a brightness temperature of 120 K determined by comparison with Titan, whose submillimeter spectrum is better known (Mark Gurwell, private communication). The overall flux scale is unlikely to be more accurate than 30%. Images were made with a variety of weighting schemes that provided slightly different angular resolutions, sensitivities, and synthesized beam sidelobe patterns.

### 3. Results and Discussion

#### 3.1. Spectrum at Image Center

Figure 1 shows the spectrum from the center of the image cube for the full USB correlator band, averaging groups of 8 channels, corresponding to a velocity width of  $2.85 \text{ km s}^{-1}$ . The CS J=14–13 line is the prominent feature centered at  $-26 \text{ km s}^{-1}$  and an approximate width at zero power of  $\sim 30 \text{ km s}^{-1}$ , values which are consistent with the systemic velocity of the source and the expansion velocity of the envelope, respectively. The line shape is difficult to interpret because spatial filtering by the interferometer results in missing flux that varies with velocity across the profile (see §3.3). The peak brightness temperature of the line at the full angular resolution of the data is well over 100 K. An additional feature appears in the spectrum near  $-100 \text{ km s}^{-1}$  with a double peaked line shape and an approximate width consistent with the circumstellar expansion. A search of the JPL spectral line catalog suggests a tentative identification of this feature with the  $\text{C}_3\text{H}_2$  8(4,4) – 7(3,5) line at 685.6125565 GHz. This species was previously detected in transitions at lower frequencies (Kawaguchi et al. 1995, Cernicharo et al. 2000). No alternative candidates line were found in the catalog of Cernicharo et al. (2000) that contains 1050 molecular species (Cernicharo, private communication). If the assignment is correct, then the line might be thought to emerge from the external shell where various carbon chain radicals are found (Guelin et al. 1993). This feature appears to be spatially compact, though, which perhaps renders the identification problematic.

#### 3.2. Continuum Emission

Figure 2 shows the continuum image obtained from the channels free of strong line emission. Visibilities from both sidebands, separated by 10 GHz, were combined in a multifrequency synthesis, resulting in an effective frequency of 680 GHz. The continuum peak position is consistent with previous determinations, in particular the 95 GHz observation from the IRAM PdBI (Guelin et al. 1993), which is marked by the cross. The peak continuum flux is 3.8 Jy, with an uncertainty dominated by systematic effects.

Previous bolometer observations of IRC+10216 at  $450 \mu\text{m}$  indicate that the SMA recovers approximately 20% of the broadband flux at this wavelength. Sandell (1994) noted that IRC+10216 has long period variations in the submillimeter and found  $19 \pm 3 \text{ Jy}$  in an  $18''$  aperture near the 635 day maximum. Jenness et al. (2002) analyzed several years of SCUBA observations of IRC+10216 at  $850 \mu\text{m}$  and  $450 \mu\text{m}$  and found a period and maximum flux consistent with the earlier single pixel measurements. The SMA observations were made

approximately a month before the predicted maximum, when  $\sim 95\%$  of the peak flux would be expected. Remarkably, the CS J=14–13 line emission *alone* accounts for 1% of the flux in the  $\sim 68$  GHz wide filter used for the 450  $\mu\text{m}$  bolometer measurements. Given the many strong spectral lines excited in the inner envelope at these high frequencies, it is clear that spectral line emission makes an important contribution to the broadband “continuum” flux.

A large fraction of the continuum emission from the compact component detected by the SMA at 680 GHz likely comes from the stellar photosphere. Lucas & Guelin (1999) report a “point source” component in IRAM PdBI observations of  $65 \pm 1$  mJy at 89 GHz and  $486 \pm 7$  mJy at 242 GHz, identified as photospheric emission. Assuming an optically thick spectrum,  $S_\nu \propto \nu^2$ , an extrapolation to 680 GHz gives 3.8 Jy, consistent with the measured value. Thermal emission from dust in the inner envelope cannot contribute substantial additional flux in the small synthesized beam of the SMA at this high frequency.

### 3.3. CS J=14–13 Emission

Figure 3 shows images for a series of velocity intervals that span the CS J=14–13 line. Below each of the images is a plot of visibility amplitude vs.  $(u, v)$  distance for the corresponding velocity interval to give an idea of spatial extent, which is not easy to ascertain from the images. The overall structure in the visibility amplitudes is consistent with simple expectations for a spherically expanding envelope. At the extreme velocities, the amplitude is approximately constant, as expected for the unresolved “caps” of blueshifted and redshifted emission, while at intermediate velocities, the fall-off of visibility amplitude with  $(u, v)$  distance demonstrates that the emission is spatially extended and resolved. If the gas is expanding radially with approximately spherical symmetry, then the narrow velocity interval around the central velocity corresponds to a cross section through the envelope in the plane of the sky.

The central peak of CS J=14–13 emission distribution provides additional direct evidence that CS is “parent” molecule, in accord with the detection of ro-vibrational transitions in absorption in the infrared (Keady & Ridgeway 1993), the detection of vibrationally excited CS emission (Turner 1987, Lucas & Guelin 1999, Highberger et al. 2000), and interferometric imaging of CS J=2–1 emission (Lucas et al. 1995). The CS molecules must originate close to the stellar photosphere, and they are lost from the expanding envelope through reactions that build more complex species, perhaps aided by shocks as suggested by Willacy & Cherchneff (1998). The J=14–13 emission distribution shows no indication of the extended  $\sim 15''$  radius ring visible in the J=2–1 line, but emission on that size scale, if present, could not be detected on account of the small SMA field of view.

The reaction network for sulfur bearing carbon chains has been explored by Millar, Flores & Markwick (2001), who concluded that an initial CS abundance of  $4 \times 10^{-6}$  is needed to match observations of C<sub>3</sub>S and C<sub>5</sub>S. Models where CS is not a parent species, in which the CS fractional abundance rises from  $< 10^{-11}$  at radius  $10^{16}$  cm, or 4''5 at 150 pc, to a peak more than four orders of magnitude larger at radius  $10^{17}$  cm, could not match observations of the longer carbon chains. The SMA observations provide a robust *lower limit* to the CS abundance within a radius of  $\sim 34 R_*$  ( $2.25 \times 10^{15}$  cm) that supports the parent species scenario. Under the assumption of a thermalized level population, the total CS column density is given by

$$N(\text{CS}) = \frac{3kf}{8\pi^3 B \mu^2} \frac{\exp(hB J_l(J_l + 1)/kT)}{J_l + 1} \frac{T + hB/3k}{1 - \exp(-h\nu/kT)} \int \tau dv, \quad (1)$$

where the molecular constants are  $\mu = 1.96$  Debye,  $B = 24.584$  GHz, and the filling factor  $f$  may be estimated as (e.g. Scoville et al. 1986)

$$f = \frac{T_R^*/\eta_c}{(h\nu/k)/(\exp(h\nu/kT) - 1)(1 - \exp -\tau)}. \quad (2)$$

The lower limit to the line flux in a  $\sim 2''$  beam is  $\sim 5000$  Jy km s<sup>-1</sup>, or  $\sim 1250$  K km s<sup>-1</sup> in brightness units. Assuming small optical depth,  $\tau \ll 1$ , a kinetic temperature equal to the excitation of the upper level of the observed transition (246.8 K), which minimizes the column density required to explain the observed line flux, and a spherical volume with molecular hydrogen density equal to the critical density of the transition of  $3.2 \times 10^8$  cm<sup>-3</sup>, results in a lower limit to the CS fractional abundance of  $\sim 3.4 \times 10^{-9}$ . The abundance close to the photosphere is likely substantially higher than this estimate; Highberger et al. (2000) derive  $3 - 7 \times 10^{-5}$  at a radius  $\sim 14 R_*$  ( $9 \times 10^{14}$  cm) from their multi-transition single dish observations. Though the uncertainties are large, models such as those investigated by Millar et al. (2001) where the CS abundance rises from  $< 10^{-11}$  at radius  $10^{16}$  cm are clearly in conflict with the high resolution images of the CS J=14–13 emission.

The SMA observations show directly that the CS molecules are formed close to the stellar photosphere. Detailed radiative transfer models that account for the observed spatial distribution are needed for an accurate determination of the CS abundance in the inner envelope. The effect of pulsational shocks could be important in establishing the CS abundance as this species is injected into the wind, and careful modeling may provide insight and constraints on the shock chemistry.

Imaging the CS J=14–13 line in the inner envelope of IRC+10216 offers a first demonstration of the efficacy of the SMA in the semi-transparent 450  $\mu$ m atmospheric window. Calibration at these high frequencies should become considerably easier as more receivers

for these frequencies are deployed at the SMA, the correlator bandwidth is increased to 2 GHz, and simultaneous operation of a lower frequency band enables phase transfer. Many more evolved stars, as well as other objects detected but with presently unresolved emission at short submillimeter wavelengths, are now accessible to imaging at the arcsecond scale.

We thank all of members of the SMA Team that made these observations possible. We thank John Bieging and the referee Jose Cernicharo for very helpful comments. We extend special thanks to those of Hawaiian ancestry on whose sacred mountain we are privileged to be guests.

## REFERENCES

- Avery, L.W. et al. 1992, ApJS, 83, 363
- Bieging, J.H., Tafalla, M. 1993, AJ, 105, 576
- Carlstrom, J.E., Hills, R.E., Lay, O.P., Force, B., Hall, C.G., Phillips, T.G., Schinckel, A.E. 1994, in *Astronomy with Millimeter and Submillimeter Wave Interferometry*, IAU Colloquium 140, eds. M. Ishiguro and J. Welch, ASP Conference Series, Vol. 59, p.35
- Cernicharo, J., Guelin, M., Kahane, C. 2000, A&AS, 142, 181
- Crosas, M., Menten, K.M. 1997, ApJ, 483, 913
- Gottlieb, C.A., Myers, P.C., Thaddeus, P. 2003, ApJ, 588, 655
- Fong, D., Meixner, M., Shah, R.Y. 2003, ApJ, 582, L39
- Groesbeck T.D., Phillips T.G., Blake, Geoffrey A., 1994, ApJS, 94, 187
- Guelin, M., Lucas, R., Cernicharo, J. 1993, A&A, 280, L19
- Highberger, J.L., Apponi, A.J., Bieging, J.H., Ziurys, L.M., Mangum, J.G. 2000, ApJ, 544, 881
- Ho, P.T.P, Moran, J.M., Lo, K.Y. 2004, ApJ, submitted
- Kawaguchi, K., Kasai, Y., Ishikawa, S.-I., Kaifu, N. 1995, PASJ, 47, 853
- Keady, J.J. & Ridgeway, S.T. 1993, ApJ, 406, 199
- Lucas, R., Guelin, M. 1999, IAU Symp. 191, Asymptotic Giant Branch Stars, eds. T LeBetre, A Lebre, C Waelkens (San Francisco: ASP), p. 305
- Lucas, R., Guelin, M., Kahane, C., Audinos, P, Cernicharo, J. 1995, Ap&SS, 224, 293
- Mauron, N. & Huggins, P.J. 1999, A&A, 349, 203
- Millar, T.J., Flores, J.R., Markwick, A.J. 2001, MNRAS, 327, 1173
- Scoville, N.Z., Sargent, A.I., Sanders, D.B., Claussen, M.J., Masson, C.R., Lo, K.Y., Phillips, T. G. 1986, ApJ, 303, 416
- Turner, B.E. 1987, A&A, 182, L15
- Willacy, K., Cherchneff, I. 1998, A&A, 330, 676



Table 1. IRC+10216 Observational Parameters

Parameter	Value
Observations:	2002 Dec 10 (3 antennas)
Min/Max baseline:	14 to 25 meters
Pointing center (J2000):	$\alpha = 9^h 47^m 57^s.39$ , $\delta = 13^h 16^m 43^s.90$
Calibrator (flux):	Callisto (56 Jy)
Primary beam HPBW:	17''
Synthesized beam HPBW:	2''3 $\times$ 1''5 P.A. 28°
K/Jy:	0.76
Spectral Line Correlator:	4 $\times$ 128 channels
usable bandwidth:	328 MHz
species/transition:	CS J=14–13
frequency:	685.435923 GHz <sup>a</sup>
channel spacing:	0.36 km s <sup>-1</sup>
r.m.s. (line images):	8 Jy beam <sup>-1</sup>

<sup>a</sup>Gottlieb, Myers & Thaddeus 2003

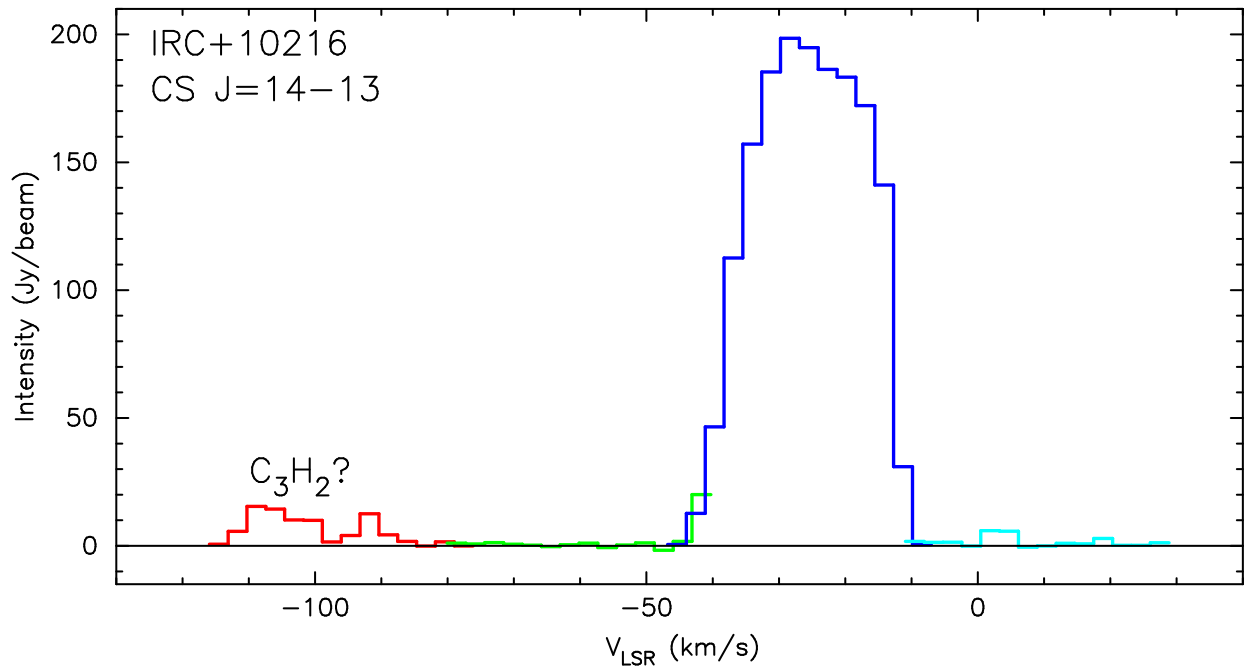


Fig. 1.— Spectrum of IRC+10216 across the full bandwidth, showing the four overlapping 104 MHz correlator “chunks”, binned to  $2.8 \text{ km s}^{-1}$  resolution, in a  $4''.6 \times 1''.6$  p.a.  $-68^\circ$  synthesized beam. Strong CS J=14–13 line emission is visible, as well as an interloping line at low velocities, tentatively identified as  $\text{C}_3\text{H}_2$ .

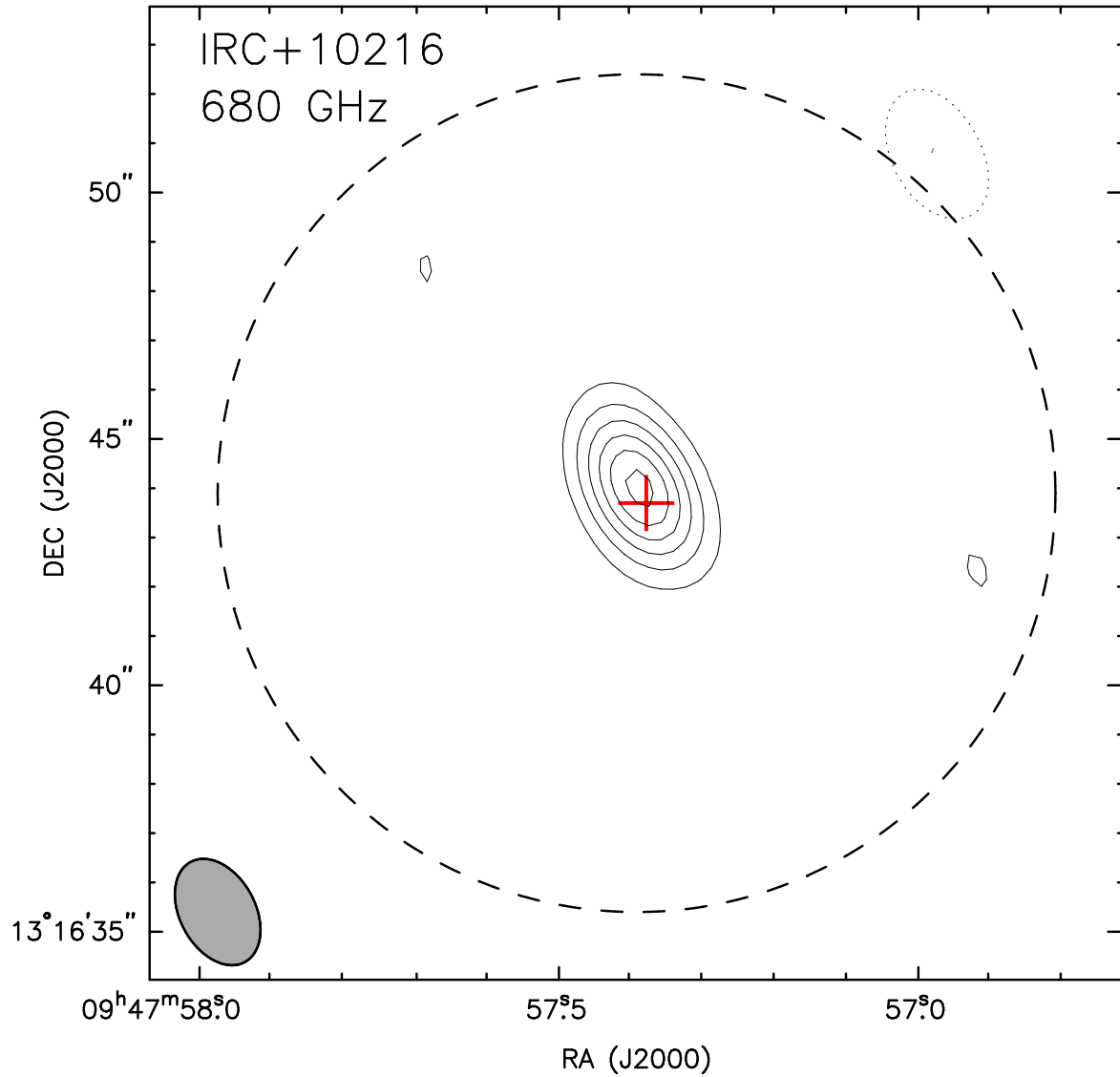


Fig. 2.— IRC+10216 continuum emission at 685 GHz. The contour levels are  $\pm 2, 4, 6, \dots \times 0.3 \text{ Jy beam}^{-1}$ . Negative contours are dotted. The ellipse in the lower left corner shows the  $2.3 \times 1.5$  p.a.  $28^\circ$  synthesized beam. The dashed circle indicates the  $17''$  FWHM primary beam size.

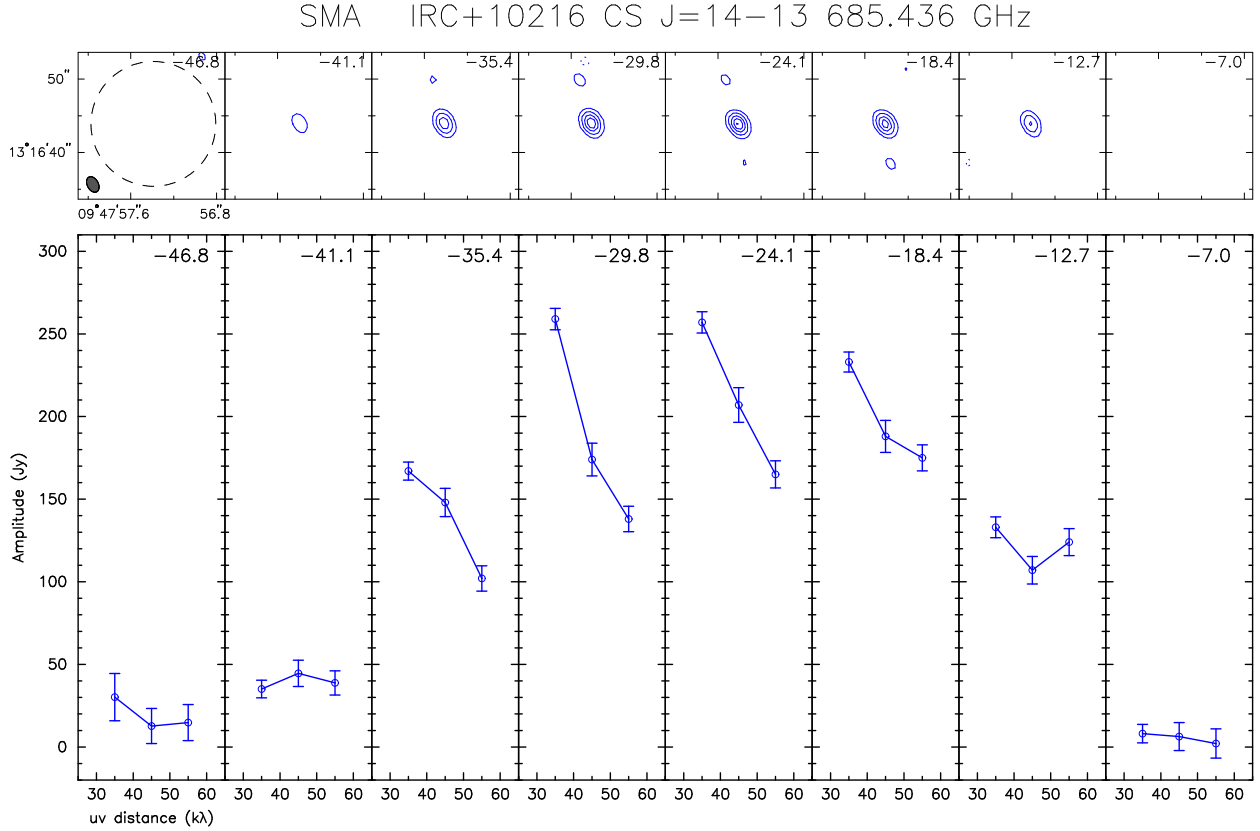


Fig. 3.— *upper*: Velocity channel maps (width  $5.7 \text{ km s}^{-1}$ ) of CS J=14–13 line emission from IRC+10216. The contour levels are  $\pm 1, 3, 6, 9, \dots \times 15 \text{ Jy beam}^{-1}$ . Negative contours are dotted. The ellipse in the lower left corner of the leftmost panel shows the  $2''.3 \times 1''.5$  p.a.  $28^\circ$  synthesized beam. The dashed circle indicates the  $17''$  FWHM primary beam size. *lower*: Visibility amplitude of the CS J=14–13 emission vs. baseline length, for the same velocity channels, annularly averaged in  $10 \text{ k}\lambda$  bins. The error bars represent  $\pm 1$  standard deviation for each bin. The falloff of amplitude with baseline length shows that the emission is spatially resolved at the central velocities, as expected for a symmetrically expanding source.